Springer

KSME

Journal of Mechanical Science and Technology 29 (8) (2015) 3165~3173
www.springerlink.com/content/1738-494x(Print)/1976-3824(Online)
DOI 10.1007/s12206-015-0715-8

Sensitive method for detecting tooth faults in gearboxes based on wavelet denoising and empirical mode decomposition †

Shuai Jin, Jong-Sik Kim and Sang-Kwon Lee*

School of Mechanical Engineering, Inha University, Inchon, 402-751, Korea

(Manuscript Received November 12, 2014; Revised March 9, 2015; Accepted April 10, 2015)

Abstract

Many signal processing methods have been developed to detect gear system faults. However, signal noise greatly influences the monitoring process. In addition, useful fatigue information can be misinterpreted by other useless oscillation components in vibration signal and noise. These conditions lead to unclear results that hinder researchers from effectively detecting faults. To overcome this problem, this study first adopts wavelet theory to remove noise and then utilizes the empirical mode decomposition characteristics of the Hilbert-Huang transform to analyze useful Intrinsic mode functions (IMFs) on the basis of signal modulation and correlation theory. Sifted IMFs are then reconstructed as new signals called D-E signals. Finally, Hilbert energy spectrum and kurtosis value are used to complete fault diagnosis. This study compares the proposed method with the Discrete wavelet transform (DWT) method to verify the superiority of the proposed method. Experiment results from using different degrees of gear crack demonstrate that the proposed method is more sensitive in gear fault detection than the DWT method.

Keywords: Wavelet denoising; Empirical mode decomposition; Intrinsic mode function; Discrete wavelet transform; Correlation; Energy; Kurtosis

1. Introduction

The gear system is an important component of a mechanical transmission system. The failure of the gear system damages machine equipment and causes economic losses. Therefore, detecting gear faults efficiently and correctly is significant. Gear diagnosis technology has been developed through many methods. As a main representative method, the signal processing method is important in detecting machine faults.

Gear systems are normally dominated by regular components. Gear speed and load are almost constant. Gear stress and stiffness change during certain failures, such as pitting, wear, scoring, and broken teeth. These changes can result in fluctuating forces, which are not characteristic of healthy machine conditions.

Analyzing vibration signals is one of the important steps in signal processing. Such analysis is appropriate when monitoring gearboxes because any change in the vibration signature of a gearbox is most likely caused by an altered gearbox condition. This is because gear defects alter both the amplitude and phase modulations of gear vibrations. Transient components caused by short duration events, such as repeated impacts, occur when certain faults exist on gears. The faults produced alter amplitude and energy [1]. Fig. 1 shows a simple physical explanation for signal processing.

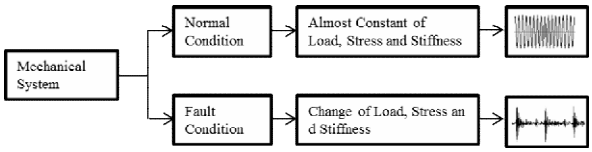

Fig. 1. Diagram of the physical explanation behind signal processing.

Fourier transform has greatly contributed to the field of health monitoring. Fourier transform is known as a comprehensive signal analysis method, but it cannot reflect local time events and the distribution of these events. Nevertheless, instantaneous parameters are important information that indicates faults [2]. Such disadvantage can be overcome with time-frequency analysis, which facilitates the identification of frequency changes with time and the effective extraction of local information. As one of the representatives of various time-frequency methods, wavelet theory has been developed and used widely [3]. The wavelet analysis method provides excellent localization analysis from the time-frequency domain of non-stationary signals. This method can reflect local signal characteristics and extract instantaneous information from signals. Additionally, the wavelet method is a multiscale analysis that is performed through scaling and translation [4]. The present study uses these advantages to accomplish

*Corresponding author. Tel.: +82 32 860 7305, Fax.: +82 32 868 1716
E-mail address: sangkwon@inha.ac.kr
† Recommended by Associate Editor Cheolung Cheong

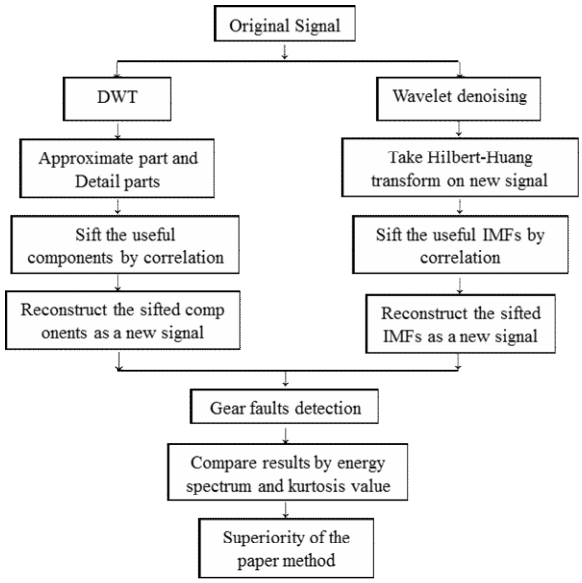

Fig. 2. Analysis process flow chart.

denoising.

Discrete wavelet transform (DWT) also draws significant attention in the condition monitoring field. However, DWT still has disadvantages, including interference terms, border distortion, and energy leakage, all of which generate certain undesired spikes across frequency scales and yield confusing results that are difficult to interpret [5].

Not all oscillation components in vibration signals contain fatigue information. Useless parts can be mixed with useful parts, and such mix complicates results [6]. This study uses the Hilbert-Huang transform (HHT) proposed by Huang et al. (1998) to retain useful components and obtain clear results. The HHT consists of Empirical mode decomposition (EMD) and Hilbert transform [7]. As the main part of the HHT, EMD produces a series of oscillatory functions called Intrinsic mode functions (IMFs) and a residual component after a specific algorithm. Certain IMFs with low frequency and low energy usually lack useful information [8]. Moreover, a large amount of time is required to analyze all IMFs. The results are also unclear for researchers to analyze. Therefore, this research combines the characteristics of EMD and correlation theory to sift useful IMFs that are highly correlated with denoising signals. The sifted IMFs are then reconstructed as new signals called D-E signals. These D-E signals focus on gear fault detection by analyzing the Hilbert energy spectrum. Finally, the kurtosis parameter shows that the proposed method is sensitive in fault detection.

The method used in this study is compared with DWT to verify the superiority of the proposed method. This comparison focuses on the vibration signal, Hilbert energy spectrum, and kurtosis value of both methods. A gearbox experiment is also performed using a healthy gear and gears with three crack degrees: small crack, big crack, and tooth cut. The final experiment results show that the proposed method can identify useful IMFs more effectively and complete gear fault detection more efficiently and accurately than the DWT method.

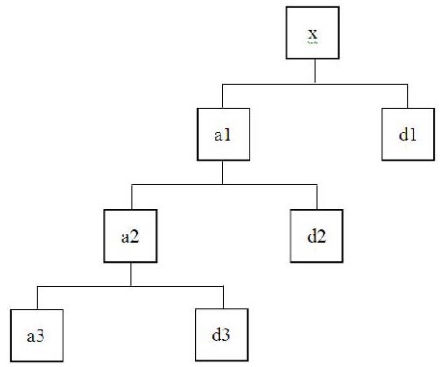

Fig. 3. Wavelet decomposition process diagram.

The rest of the paper is organized as follows. Sec. 2 discusses wavelet denoising theory and the steps involved in wavelet denoising. Sec. 3 briefly introduces DWT. The EMD algorithm and Hilbert spectral analysis are also introduced. Sec. 4 presents the cross-correlation coefficient assumption and equation. Sec. 5 illustrates kurtosis theory. Sec. 6 introduces the experiment rigs and specifications. The experiment results are then analyzed. Finally, Sec. 7 presents the conclusion. The flow chart of the analysis process is shown in Fig. 2.

2. Wavelet denoising

2.1 Wavelet denoising theory

A common denoising problem model is as follows [9]:

$$y_i = f_i + \sigma z_i \tag{1}$$

where y_i is the signal with noise and f_i is the clean signal without noise. z_i is the independent, identically distributed Gaussian white noise ($z_i \sim^{iid} N(0,1)$); and σ is the noise level. This study utilizes the different characteristics between the clean signal and noise under wavelet transform to separate the signal and noise on the basis of wavelet decomposition coefficients.

The wavelet decomposition on the signal with noise is as follows [10]. The number of decomposition levels is assumed to be 3.

$$x = a_1 + d_1 = a_2 + d_2 + d_1 = a_3 + d_3 + d_2 + d_1 \tag{2}$$

where a_i is the approximate part of the decomposition and d_i is the detail part of the decomposition ($i = 1,2,3$). Approximates correspond to low frequency components while details contain high frequency components. The process diagram is shown in Fig. 3.

A wavelet threshold is then used to solve the wavelet coefficient and to reconstruct the signal. Thresholding wavelet coefficients are applied to the detail coefficients instead of the approximation coefficients, given that the approximation part

usually contains important signal information.

2.2 Wavelet denoising steps

In this study, wavelet denoising is divided into three parts.

(1) Wavelet decomposition on the acquisition data. The signal model is expressed as Eq. (1).

(2) Thresholding of wavelet coefficients. This study uses the famous threshold form proposed by Donoho et al. The equation is expressed as follows [11]:

$$t_n = \sigma\sqrt{2\log n}. \tag{3}$$

When n approaches infinity, signal noise can almost be completely removed. Given the large data length used this study, Eq. (3) is adopted to obtain the threshold value.

Next, threshold is assigned on the basis of the modified detail coefficients. Soft thresholding provides smoother results compared with hard thresholding. Eq. (3) is also solved through soft thresholding, which can obtain excellent denoising effects [12]. Soft thresholding is expressed as follows:

$$\eta_s = (w,t) = \begin{cases} w - t, w \geq t \\ 0, |w| < t \\ w + t, w \leq t. \end{cases} \tag{4}$$

(3) Signal reconstruction after inverse transformation of processed wavelet coefficients. The formula combined with Eq. (1) is as follows [13]:

$$f_n = w_0^{-1}\eta_s w_0 d \tag{5}$$

where f_n is the new signal after denoising and w_0 is the wavelet coefficient.

3. DWT and Hilbert-Huang transform

3.1 A brief introduction to DWT

Given the wide use of the DWT method, it is introduced briefly in this section. DWT is any wavelet transform for which wavelets are discretely sampled. DWT decomposes signals into different frequency bandwidths. DWT can be expressed as [14]

$$T_{m,n} = \int x(t) a_0^{-m/2} \psi(a_0^{-m/2} t - n b_0) dt \tag{6}$$

where $x(t)$ is the analyzed signal, ψ is the mother wavelet a_0^m, $m \in Z$ is the dilation parameter discretization, and b_0 is the translated step. A vibration signal contains different components, and the distribution of fault components after wavelet decomposition differs in each scale [15]. The DWT results are divided into the low-frequency approximate part and the high-frequency detail part.

3.2 EMD algorithm

The EMD process is based on the assumption that a signal involves several IMFs and a residual. Each IMF should satisfy two conditions: (1) the number of extrema and the number of zero crossing in a dataset should either be equal or differ at most by one; (2) the mean value of the envelope is defined by the local maxima, and the envelope defined by the local minima is zero at any point. Each IMF is independent and can be both amplitude and frequency modulated. The EMD method can decompose any time-series signal $x(t)$ according to the assumptions. The details of the decomposition algorithm are as follows [16]:

(1) All the local extreme point values in a signal are determined, and cubic spline interpolation function is used to fit the upper and lower signal envelopes.

(2) The mean value of the upper and lower envelopes is designated as m_1. The first component of the difference between data $x(t)$ and m_1 is expressed as h_1, that is,

$$h_1 = x(t) - m_1. \tag{7}$$

(3) Whether h_1 is an IMF is determined. If h_1 is not an IMF, then h_1 is regarded as the original signal to repeat step 1. The mean value of the upper and lower envelopes of h_1 is expressed as m_{11}. Similar to Eq. (5), a new signal component is calculated as

$$h_{11} = h_1 - m_{11}. \tag{8}$$

(4) The algorithm is repeated k times until h_{1k} satisfies the two IMF conditions. The first IMF component is denoted as C_1.

(5) C_1 is extracted from $x(t)$, and the first residue r_1 is obtained.

$$r_1 = x(t) - C_1. \tag{9}$$

(6) Residue r1 is regarded as the original signal to repeat the above sifting process. After n times of sifting, the algorithm can be stopped if residue r_n is constant or a monotonic function.

(7) Finally, the original signal $x(t)$ can be expressed as

$$x(t) = \sum_{i=1}^{n} C_i + r_n. \tag{10}$$

The residue component does not actually require analysis because this component is a trend or a constant, which contains minimal useful information.

3.3 Hilbert spectral analysis

The second part of the HHT is Hilbert transform. The Hil-

bert transform $y_i(t)$ of one of the IMFs (C_i) in Eq. (9) can be defined as

$$y_i(t) = \frac{1}{\pi} P \int_{-\infty}^{\infty} \frac{C_i(t')}{t - t'} dt' \tag{11}$$

where P is the Cauchy principal value of the singular integral. The analytic function can be obtained through Eq. (5) as follows:

$$z_i(t) = C_i(t) + jy_i(t) = a_i(t) e^{j\theta_i(t)} \tag{12}$$

where $j = \sqrt{-1}$, $a_i(t) = \sqrt{C_i^2(t) + y_i^2(t)}$, $\theta_i(t) = \arctan \frac{y_i(t)}{C_i(t)}$.

The instantaneous frequency can be expressed as follows on the basis of the instantaneous phase function $\theta_i(t)$:

$$\omega_i(t) = \frac{d\theta_i(t)}{dt}. \tag{13}$$

The Hilbert-Huang spectrum $H(\omega, t)$ is the time-frequency distribution with both amplitude and frequency as functions of time. From $H(\omega, t)$, the marginal spectrum $h(\omega)$ is expressed as

$$h(\omega) = \int_0^T H(\omega, t) dt \tag{14}$$

where T is the total data length. In addition to $h(\omega)$, instantaneous energy *IE(t)* is expressed as [7]

$$IE(t) = \int_{\omega_1}^{\omega_2} H^2(\omega, t) d\omega. \tag{15}$$

According to Eq. (14), *IE* is a function of time and is used to check energy fluctuations.

4. Cross correlation

The original signal *x(t)* is assumed to be at time t_1, and any one of the IMFs is *C(t)* at time t_2. Time delay τ is defined as $\tau = t_2 - t_1$. The cross-correlation coefficient is defined as [17]

$$\rho_{xy} = \frac{C_{xc}(\tau)}{\sigma_x \sigma_c} \tag{16}$$

where $C_{xc}(\tau)$ is the cross covariance of *x(t)* and *C(t)*, σ_x is the standard variance of *x(t)*, and σ_c is the standard variance of *C(t)*.

x(t) and *C(t)* are fully related when $|\rho_{xc}| = 1$. If *x(t)* and *C(t)* are uncorrelated, then $|\rho_{xc}| = 0$. The cross-correlation coefficient value is high and close to 1, and signals *x(t)* and *C(t)* are highly correlated. Therefore, an IMF component with high correlation preserves the most denoising signal information.

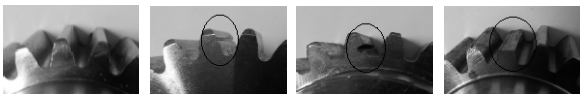

(a) (b) (c) (d)

Fig. 4. Gear conditions: (a) healthy; (b) small crack; (c) big crack; (d) tooth cut.

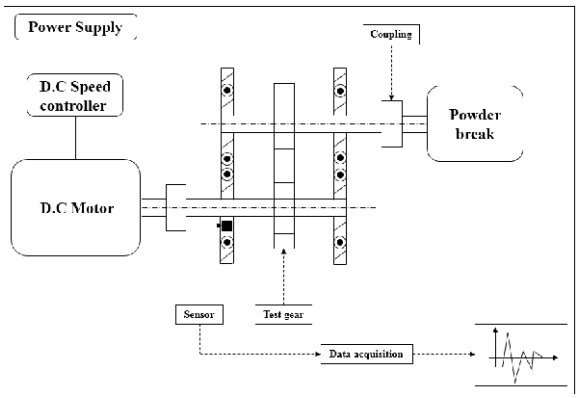

Fig. 5. Experiment rig.

5. Kurtosis

Kurtosis is the degree of peakedness of a distribution. Its coefficient is defined as

$$kurt = \frac{E[(X - \mu_x)^4]}{\sigma_x^4} = \frac{(\mu_x)_4}{\sigma_x^4} \tag{17}$$

where $(\mu_x)_4$ is the fourth moment of the mean of a signal and σ_x is the standard deviation of a signal [18].

Kurtosis describes how peaked or flat a distribution is. Kurtosis is widely used as a measure in machinery condition monitoring; for example, early damage in the rolling elements of a machinery often results in vibrator signals, the kurtosis value of which significantly increases because of faults in such rotating system [17].

6. Experiment

6.1 Experiment rigs

The gears used in the experiment consist of a healthy gear and gears with three crack degrees: small crack, big crack, and tooth cut. The cracked gear conditions are shown in Fig. 4.

The experiment rig consists of a 0.75 KW DC motor and a single-stage spur gear on two parallel shafts, as shown in Fig. 5.

The crack is located on a driving gear with 24 teeth while the driving gear has 25 teeth. Table 1 presents the detailed experiment specifications.

A speed controller connected to the input shaft controls the rotation speed. Torque load is provided to the gearbox from the eddy current magnetic brake. The device has a maximum torque capacity of 12 Nm. Vibration signals are acquired by

Table 1. Experiment specification.

Parameters	Pinion	Gear
Number of teeth	24	25
Deport angle	0.00	0.00
Pressure angle	20°	20°
Height	6.53	6.53
Module	3	3
Face width	30	30
Pitch diameter	72.72	75.75
Diameter of base	68.34	71.18
Diameter of head	78.78	81.81

Table 2. Cross-correlation coefficient values between the original signal and DWT results for the small crack gear.

Value	a4	d4	d3	d2	d1
Orig.	0.2484	0.3263	0.6166	0.6100	0.2800

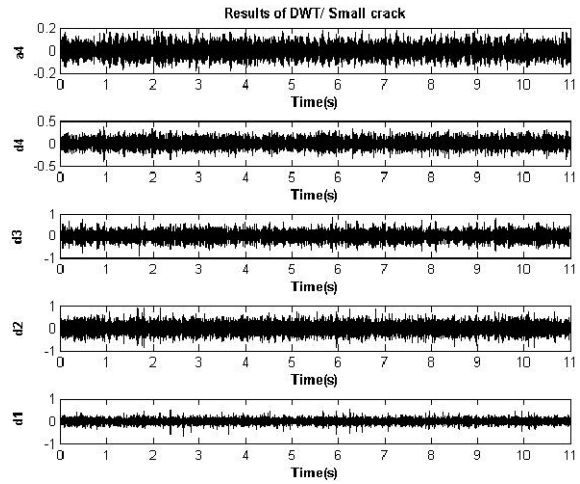

Fig. 6. DWT results for the small crack gear.

using a Bruel and Kjaer 4506 triaxial accelerometer on the input shaft bearing housing. Signal acquisitions are conducted using an LMS Mobile and are sampled at 8.2 KHz.

6.2 Results analysis

6.2.1 Sifting useful signal components

For the DWT method, this study uses db10 wavelet and four decomposition steps. The results for the small crack gear are shown in Fig. 6, which presents the approximate part of the fourth decomposition a4. The other components are detail components from the first to fourth decompositions d1-d4. The cross correlation between the DWT results and original signal is used as evaluation criteria to determine the useful components. The correlation coefficients are presented in Table 3. In Table 3, d2 and d3 have a high correlation with the original signal, which means that these decompositions contain a large amount of useful information. Then, d2 and d3 are reconstructed as reconstruction signals.

Table 3. Cross-correlation coefficient values between the original signal and DWT results for the healthy gear.

Value	a4	d4	d3	d2	d1
Orig.	0.1336	0.7489	0.5139	0.3762	0.1257

Table 4. Cross-correlation coefficient values between the original signal and DWT results for the big crack gear.

Value	a4	d4	d3	d2	d1
Orig.	0.1246	0.3049	0.6143	0.6313	0.3401

Table 5. Cross-correlation coefficient values between the original signal and DWT results for the tooth cut gear.

Value	a4	d4	d3	d2	d1
Orig.	0.2333	0.3079	0.6510	0.6008	0.2571

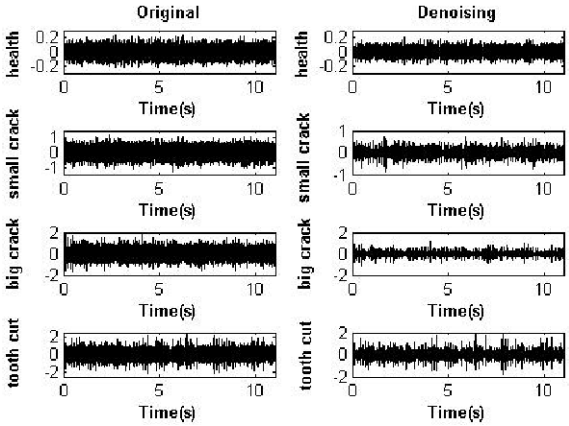

Fig. 7. Original and denoising signals of the four types of gears.

The steps involved in the analysis of the healthy, big crack, and tooth cut gears are similar to those in the analysis of small crack gears. For the three gear types, the cross-correlation coefficient results are stated directly in Tables 3-5. The first two components with the highest correlation with the original signal in Tables 4-6 are chosen to be reconstructed as reconstruction signals.

The rotational speed of the pinion axis is 420 rpm. Therefore, the duration of one cycle is 0.1429 s. The original vibration signal and wavelet denoising signal of the four gears are shown in Fig. 7. This study uses Root mean square error (RMSE) and signal-to-noise ratio (SNR) to verify the denoising results for each wavelet denoising [16, 19]. RMSE and SNR are important indicators in verifying the effect of signal denoising. The RMSE and SNR values for the denoising results are presented in Table 6. Table 6 shows a small RMSE value and a large SNR value. The denoising process is thus credible. Similar to that in the DWT method, a small crack

Table 6. RMSE and SNR values for the denoising results.

Types of gear	RMSE	SNR
Healthy	2.97e-04	11.9292
Small crack	3.33e-04	45.1204
Big crack	6.85e-05	57.3285
Tooth cut	8.71e-05	34.5764

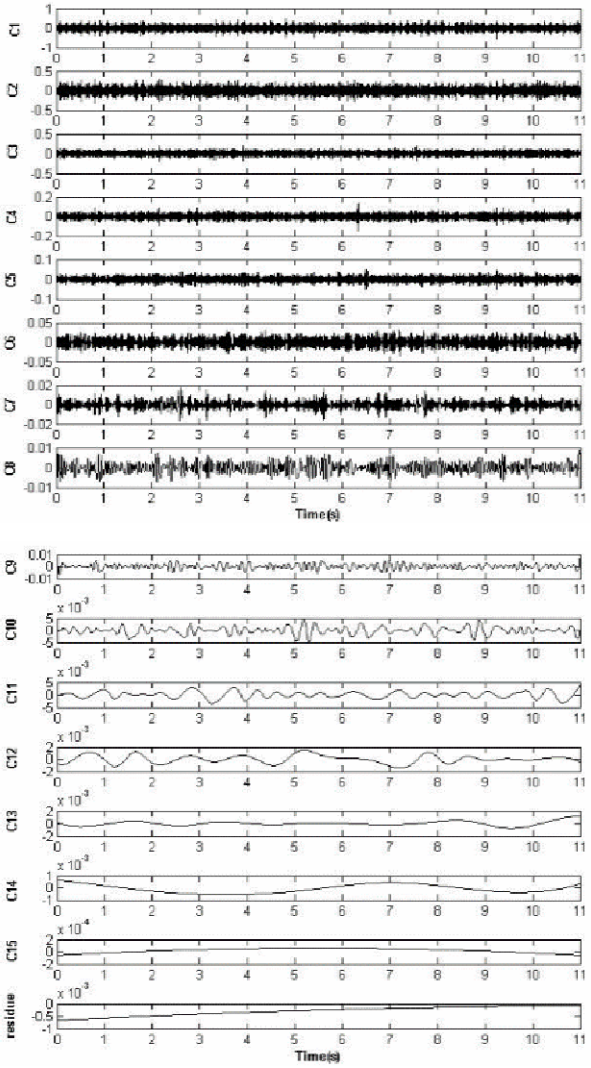

Fig. 8. EMD results of the small crack gear signal.

gear is selected for the EMD process analysis. The other gear types are directly analyzed, and the results are presented in the paper.

Fig. 8 displays the EMD results of the small crack gear vibration signal. Many IMFs occur after EMD. Hence, analyzing all IMFs and residues in research or in practical industry tasks would be time consuming. Not all IMFs actually contain useful gear damage signal information. Certain IMFs can even affect damage detection results by polluting impact information. Cross-correlation coefficients can be calculated to determine the IMFs that preserve the most information of the original signal and consequently eliminate useless IMFs. Table 7 shows the cross-correlation coefficient between the denoising signal and the IMFs. Given that the components from C9 to the residue part do not contain useful information with low frequency and low energy, the cross-correlation analysis of these components is neglected [8].

Table 7. Cross-correlation coefficient values between the Denoising signal (D.S) and the IMFs for the small crack gear.

Value	C1	C2	C3	C4
D.S	0.7391	0.3354	0.1442	0.0962
Value	C5	C6	C7	C8
D.S	0.0521	0.0293	0.0092	2.4e-005

Table 8. Cross-correlation coefficient values between the denoising signal and C1-8 for the healthy gear.

Value	C1	C2	C3	C4
D.S	0.7930	0.5303	0.0763	0.0165
Value	C5	C6	C7	C8
D.S	0.0057	3.5e-004	4.2e-004	7.5e-005

Table 9. Cross-correlation coefficient values between the denoising signal and C1-8 for the big crack gear.

Value	C1	C2	C3	C4
D.S	0.6633	0.2832	0.0498	0.0301
Value	C5	C6	C7	C8
D.S	0.0179	0.0125	0.0042	1.1e-004

Table 10. Cross-correlation coefficient values between the denoising signal and C1-8 for the tooth cut gear.

Value	C1	C2	C3	C4
D.S	0.7063	0.3800	0.1122	0.2874
Value	C5	C6	C7	C8
D.S	0.1939	0.0158	0.0022	1.7e-004

Similar to that in the DWT method, the cross-correlation coefficient results for the three gear types are shown directly in Tables 8-10.

The results in the table show that the coefficient values of C1 and C2 are higher than those of the others. The next research step focuses on C1 and C2. Fatigue crack actually affects tooth stiffness and causes load fluctuation, which changes vibration amplitude. These vibration signal changes are called amplitude and phase modulations. Modulations generally have clearer effects on high carrier frequency signals than on low carrier frequency signals. Therefore, fault information is very clear in high frequency signals [2, 20]. These clear effects also agree with the cross-correlation comparison

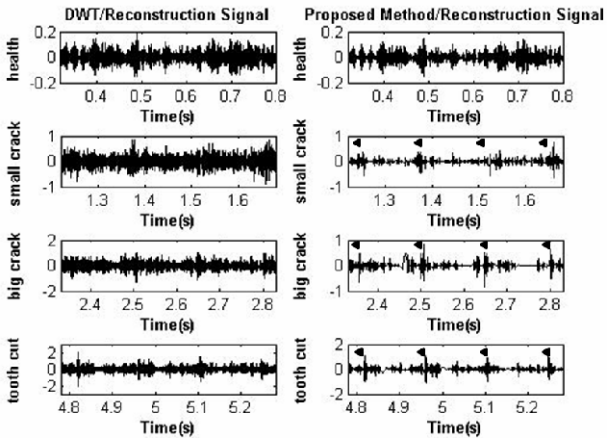

Fig. 9. Zoomed in image of the reconstruction signals via the two methods.

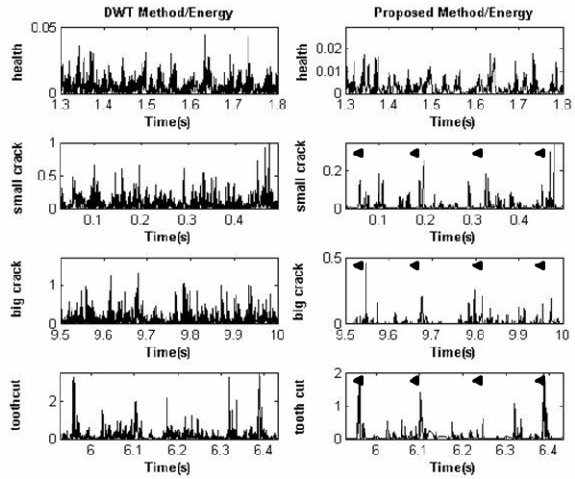

Fig. 10. Zoomed in image of the Hilbert energy spectrum via the two methods.

results. Therefore, C1 and C2 are combined to reconstruct a D-E signal.

6.2.2 Gear diagnosis

Gear diagnosis with different methods is compared according to the useful components obtained after DWT and IMF sifting based on the correlation coefficient calculation. The healthy gear is regarded as the reference of normal condition. Fig. 9 presents the reconstruction signal of the two methods.

The figure obviously shows clearer peaking impacts every 0.14 s (7 Hz) with the proposed method than with the DWT method. These periodic impacts do not appear in the healthy gear but are evident in the cracked gear for each rotation. Thus, these impacts are called fault impacts.

Fig. 10 also shows that the results of the proposed method are much clearer than those of the DWT method because EMD is an adaptive process unlike the DWT process, which depends on selected wavelets and man-made decompositions.

Table 11. Kurtosis values of the reconstruction signal obtained with DWT and the D-E signal obtained with the proposed method.

Types of gear	DWT method	Proposed method
Healthy	3.0099	3.9011
Small crack	3.6825	9.5374
Big crack	3.8666	12.6717
Tooth cut	5.3233	15.7020

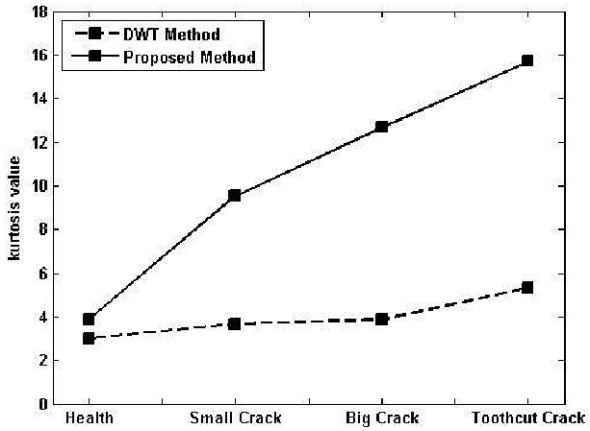

Fig. 11. Comparison of the kurtosis values of the original and D-E signals.

Additionally, IMFs are almost orthogonal and monocomponent. IMFs can capture instantaneous information more efficiently than approximate and detail parts after DWT. Energy leakage occurs after DWT and thus affects results. In addition, wavelet transform cannot achieve a fine resolution in both time and frequency domains simultaneously because of the limitation of the Heisenberg-Gabor inequality [5].

Through wavelet denoising and retention of useful oscillation components, the proposed method can detect faults sensitively. The results are shown clearly for researchers to complete their health monitoring tasks.

This study uses kurtosis parameters statistically to confirm the superiority of the proposed method. A damaged gear produces a vibration signal with sharp peaks, and then the distribution function of this gear becomes noticeably sharp. Therefore, the kurtosis value is higher for the cracked gears than for the healthy gear. Table 11 shows the kurtosis values of the reconstruction signal obtained with DWT and the D-E signal obtained with the proposed method for the four gear types. The kurtosis values are plotted in Fig. 11.

According to Table 11 and Fig. 11, the kurtosis values of the proposed method are bigger than those of the DWT method. The kurtosis values also enlarge as the crack degree increases. The kurtosis values of the proposed method are bigger than those of the DWT method because the reconstruction signal after DWT contains noise. Moreover, detail parts cannot express instantaneous features better than IMFs. Interference terms and leakage affect oscillation distributions. Im-

pact oscillations caused by a crack can be hidden in these noises, and small undesired spikes generate small kurtosis values. However, the proposed method eliminates the influence of noise and useless components and then enables the kurtosis value to reflect the actual impact distribution.

7. Conclusions

This study proposed a sensitive gear fault detection method. Wavelet theory was first utilized to complete denoising with low RMSE and high SNR. The EMD algorithm was calculated after removing the influence of noise. Many IMFs and a residue were produced after EMD. Not all the oscillations actually contained important information. This study used signal modulation and correlation theory to sift useful IMFs. These sifted IMFs were highly correlated with the original signal and were modulated in a clearer way compared with the other components. The sifted IMFs were then reconstructed into D-E signals. The D-E signals focused on gear fault detection. In the comparison of the proposed method with the DWT method, the results from the time domain vibration signal and the Hilbert energy spectrum showed that the proposed method was highly sensitive in selecting the impact information caused by a cracked gear. The kurtosis values also demonstrated the superiority of the D-E signal in damage detection. Therefore, the proposed method was regarded as sensitive and capable of effectively detecting gear fatigue. The experiment verified that the fault information of the D-E signals was clearer than that of the original signal after DWT. A method for extracting additional information from other IMFs will be explored in future works to detect gearbox faults comprehensively.

Acknowledgments

This work was supported by the Mid-career Researcher Program through a National Research Foundation grant that was funded by the Ministry of Education, Science, and Technology (No. 2010-0014260). This work was also supported by a research grant from Inha University.

References

[1] Al-Arbi and Salem, Condition monitoring of gear system using vibration analysis, *Ph.D. Thesis*, University of Huddersfield (2012).

[2] A. Belsak and J. Flasker, Wavelet analysis for gear crack identification, *Engineering Failure Analysis*, 16 (2009) 1983-1990.

[3] I. Daubechies, The wavelet transform, Time-frequency localization and signal analysis, *IEEE Trans. Inform. Theory*, 36 (6) (1990) 961-1005.

[4] C. Torrence and G. P. Compo, A practical guide to wavelet analysis, *Bull. Amer. Meteor. Soc*., 79 (1998) 61-78.

[5] Z. K. Peng, P. W. Tse and F. L. Chu, A comparison study of improved Hilbert-Huang transform and wavelet transform: Application to fault diagnosis for rolling bearing, *Mechanical Systems and Signal Processing,* 19 (2005) 974-988.

[6] Z. K. Peng, P. W. Tse and F. L. Chu, An improved Hilbert-Huang transform and its application in vibration signal analysis, *Journal of Sound and Vibration*, 286 (2005) 187-205.

[7] N. E. Huang, Z. Shen, S. R. Long, M. C. Wu and H. H. Shih, The empirical mode decomposition and Hilbert spectrum for nonlinear and non-stationary time series analysis, *Proceedings of the Royal Society of London A*, 454 (1998) 903-995.

[8] S. J. Loutridis, Damage detection in gear systems using empirical mode decomposition, *Engineering Structures*, 26 (2004) 1833-1841.

[9] S. Sylvain, T. Paul and B. Andrew, Robust wavelet denoising, *IEEE Transactions on Signal Processing*, 49 (6) (2001) 1146-1152.

[10] B. Mozaffari and M. A. Tinati, Blind source separation of speech sources in wavelet packet domains using Laplacian mixture model expectation maximization estimation in overcomplete cases, *Journal of Statistical Mechanics: Theory and Experiment*, P02004 (2007) 1-31.

[11] D. L. Donoho and I. M. Johnstone, Ideal spatial adaptation by wavelet shrinkage, *Biometrika*, 81 (1994) 425-455.

[12] D. L. Donoho, De-noising by soft-thresholding, *IEEE Trans. Inform. Theory*, 41 (1995) 613-627.

[13] N. Tomohiko and K. Hirokazu, Fast signal reconstruction from magnitude spectrogram of continuous wavelet transform based on spectrogram consistency, *Proc. of the 17th Int. Conference on Digital Audio Effects (DAFx-14)* (2014) 1-5.

[14] Ž. B. Jakovljević, Comparative analysis of Hilbert Huang and discrete wavelet transform in processing of signals obtained from the cutting process: An intermittent turning example, *FME Trans.*, 41 (2013) 342-348.

[15] Y. Guo, W. Yan and Z. Bao, Gear fault diagnosis of wind turbine based on discrete wavelet transform, *Proceedings of the 8th World Congress on Intelligent Control and Automation (WCICA'10)* (2010) 5804-5808.

[16] N. E. Huang and Z. Wu, A review on Hilbert-Huang transform: Method and its application to geophysical studies, *Review of Geophysics,* 46 (2008) 1-23.

[17] K. Shin and J. K. Hammond, *Fundamental of signal processing for sound and vibration engineers*, John Wiley & Sons, Ltd., England (2008) 131-134, 202-229.

[18] P. Vecer, M. Kreidl and R. Smid, Condition indicators for gearbox condition monitoring systems, *Acta Polytechnica*, 45 (2005) 35-43.

[19] T. Chai and R. P. Draxler, Root mean square error (RMSE) or mean absolute error (MAE)? - Arguments against avoiding RMSE in the literature, *Geoscientific Model Development*, 7 (2014) 1247-1250.

[20] K. Wang, Phase information at tooth mesh frequency for gear crack diagnosis, *Proceedings of the 2nd IEEE Conference on Industrial Electronics and Applications (ICIEA 2007)*, Harbin, China (23-25) (2007) 2712-2717.

Shuai Jin is a graduate student in the Department of Mechanical Engineering at Inha University. He studied signal processing and health monitoring.

Sang-Kwon Lee was born in Pusan, Korea, in 1959. He acquired his bachelor's degree in mechanical engineering from Pusan National University, Pusan, Korea. He received his Ph.D. degree in signal processing from the Institute of Sound and Vibration Research of Southampton University in the UK in 1998. He has accumulated 11 years of experience in automotive noise control by working with Hyundai Motor Co. and Renault-Samsung Motor Company in Korea. He moved to Inha University, Inchon, Korea in 1999. He has continued his sound and vibration research in the Department of Mechanical Engineering at Inha University.